

The inner product (I.P.) between two Bloch function ( $\mathbf{k}=\mathbf{k}'$ ) is

$$\begin{aligned} \text{I.P.} &\propto \sum_{\mathbf{b}} C_{n\mathbf{b}} C_{m\mathbf{b}}^* \\ &\propto \sum_{\mathbf{b}} \frac{\bar{v}(-\mathbf{k}-\mathbf{b})\bar{v}(\mathbf{k}+\mathbf{b})}{[(\mathbf{k}+\mathbf{b})^2-\mathcal{E}_n][(\mathbf{k}+\mathbf{b})^2-\mathcal{E}_m]} \\ &\quad \times \sum_{jj'} \exp[-i\mathbf{b}\cdot(\boldsymbol{\tau}_{1j}-\boldsymbol{\tau}_{1j'})] D_j D_{j'}^*. \quad (\text{A2}) \end{aligned}$$

Again decomposing into partial fractions, we obtain

$$\text{I.P.} \propto \frac{1}{(\mathcal{E}_m-\mathcal{E}_n)} \sum_{ii'} D_j D_{j'}^* \{\Phi_{jj'}(\mathcal{E}_m) - \Phi_{jj'}(\mathcal{E}_n)\},$$

which clearly vanishes, since the  $D_j$  are components of an eigenvector of the  $\Phi$  matrix.

## Magnetization and Electrical Resistivity of Gadolinium Single Crystals\*

H. E. NIGH, S. LEGVOLD, AND F. H. SPEDDING

*Institute for Atomic Research and Department of Physics, Iowa State University, Ames, Iowa*

(Received 25 June 1963)

The magnetic moment of single-crystal Gd has been measured in fields from 0 to 18 kOe along the  $\langle 0001 \rangle$ ,  $\langle 10\bar{1}0 \rangle$ , and  $\langle 11\bar{2}0 \rangle$  directions at temperatures from 1.4 to 900°K. Small anisotropy was observed below the Curie temperature and the easy direction of magnetization was found to be a function of temperature. The absolute saturation magnetic moment was found to be 7.55 Bohr magnetons/atom. The saturation magnetization was observed to follow the  $T^{3/2}$  law from 200 to 50°K with a deviation from this law observed below 50°K. A ferromagnetic Curie temperature of 293.2°K is reported. The effective Bohr magneton number in the paramagnetic region is 7.98 and the paramagnetic Curie temperature is 317°K. Electrical resistivity measurements were made from 4.2 to 380°K on the  $b$ -axis and  $c$ -axis crystals. For the  $b$  axis, the resistivity changes slope at 293.2°K. The  $c$  axis exhibits a small maximum at 292°K and a shallow minimum at 340°K.

### INTRODUCTION

**G**ADOLINIUM was the fourth ferromagnetic element to be discovered.<sup>1</sup> Trombe<sup>2</sup> and Elliott *et al.*<sup>3</sup> found a Curie temperature of 289°K and an absolute saturation magnetization of 7.12 Bohr magnetons/atom. Henry<sup>4</sup> found a saturation magnetization of 7.05 Bohr magnetons/atom at 1.3°K and 60 000G. Gaskell and Motz<sup>5</sup> report magnetic moments at 80 000G which are about 15% higher than those for infinite fields as extrapolated by Elliott *et al.*

Arajs and Colvin<sup>6</sup> reported a paramagnetic Curie temperature of 310°K and an effective Bohr magneton number of 8.07. They observed a small anomaly, which could be enhanced by small additions of Mo and Ta, at about 750°K.

Belov *et al.*<sup>7</sup> found a peak in the magnetic moment

at 210°K in magnetic fields of less than 1.12 Oe from measurements on a toroidal sample. The isofields below 112 Oe also showed anomalous behavior at low temperatures. In addition, they reported small kinks in the magnetization curves above 210°K. Their conclusion was that a spiral spin structure exists in Gd between 210 and 290°K.

More recently, the magnetocrystalline anisotropy of Gd has been measured by Graham<sup>8</sup> and by Corner *et al.*<sup>9</sup> They both found that above 240 to 245°K the  $c$  axis is the easy direction of magnetization. Graham reports an easy cone of magnetization between 225 and 245°K, and below about 165°K. Between 165 and 225°K he found that the easy direction of magnetization is in the basal plane. Corner *et al.* report an easy cone of magnetization from 240 to 37.5°K, the lowest temperature used. Corner found that the easy direction reaches a maximum angle of 70° with respect to the  $c$  axis at 220°K. In addition, Graham observed that low field magnetization curves were in qualitative agreement with those calculated from the anisotropy constants.

The temperature dependence of the lattice parameters of single crystal Gd has been measured recently by Darnell.<sup>10</sup> He reports a Curie temperature of 298°K.

\* Contribution No. 1322. Work was performed in the Ames Laboratory of the U. S. Atomic Energy Commission.

<sup>1</sup> G. Urbain, P. Weiss, and F. Trombe, *Compt. Rend.* **200**, 2132 (1935).

<sup>2</sup> F. Trombe, *Ann. Phys. (N. Y.)* **7**, 383 (1937).

<sup>3</sup> J. F. Elliott, S. Legvold, and F. H. Spedding, *Phys. Rev.* **91**, 28 (1953).

<sup>4</sup> W. E. Henry, *J. Appl. Phys.* **29**, 524 (1958).

<sup>5</sup> C. S. Gaskell and H. Motz, in *High Magnetic Fields* (Technology Press, Cambridge, Massachusetts, 1962; and John Wiley & Sons, Inc., New York, 1962), p. 561ff.

<sup>6</sup> S. Arajs and R. V. Colvin, *J. Appl. Phys.* **32**, 336S (1961).

<sup>7</sup> K. P. Belov, R. Z. Levitin, S. A. Nikitin, and A. V. Ped'ko, *Zh. Eksperim. i Teor. Fiz.* **4**, 1562 (1961) [translation: *Soviet Phys.—JETP* **13**, 1096 (1961)]; K. P. Belov and A. V. Ped'ko, *ibid.* **42**, 87 (1961) [translation: *ibid.* **15**, 62 (1962)].

<sup>8</sup> C. D. Graham, Jr., *J. Phys. Soc. Japan* **17**, 1310 (1962); C. D. Graham, Jr., *J. Appl. Phys.* **34**, 1341 (1963).

<sup>9</sup> W. D. Corner, W. C. Roe, and K. N. R. Taylor, *Proc. Phys. Soc. (London)* **80**, 927 (1962).

<sup>10</sup> F. J. Darnell, *Phys. Rev.* **130**, 1825 (1963).

The heat capacity of Gd has been measured over the temperature range 15 to 355°K by Griffel, *et al.*<sup>11</sup> They observed a peak in the heat capacity at 291.8°K.

Measurements of the electrical resistivity by Colvin *et al.*<sup>12</sup> revealed a sharp change in slope between 291 and 292°K.

### EXPERIMENTAL PROCEDURE

The single crystals were produced by annealing arc melted buttons using a technique previously described.<sup>13</sup> Three samples were cut from the bulk crystals in the form of rectangular parallelepipeds and were shaped with the long dimension parallel to the  $\langle 0001 \rangle$  direction

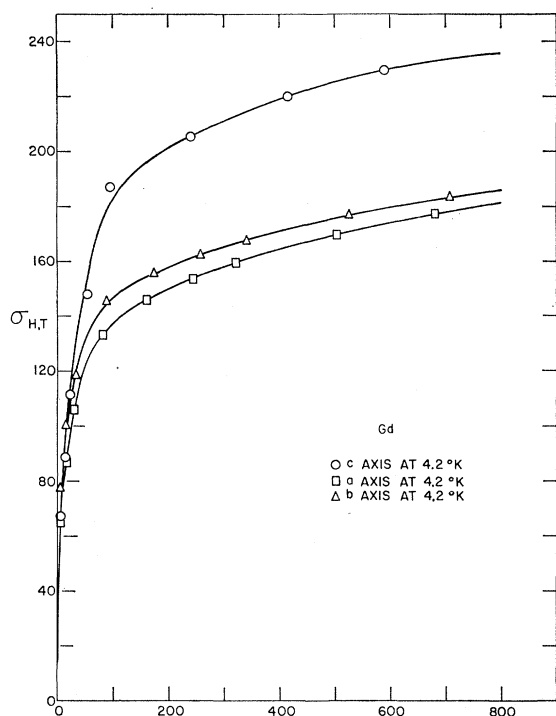


FIG. 1. Magnetic moment per gram versus internal magnetic field for the  $a$ -,  $b$ -, and  $c$ -axis crystals.

( $c$  axis),  $\langle 11\bar{2}0 \rangle$  direction ( $a$  axis), and  $\langle 10\bar{1}0 \rangle$  direction ( $b$  axis), respectively. The electrical resistivity was measured on samples 1 mm  $\times$  1 mm  $\times$  18 mm and these samples were then cut down to 1 mm  $\times$  1 mm  $\times$  10 mm for magnetic measurements from 1.3 to 300°K. The samples used for susceptibility measurements from 300 to 900°K were 2 mm  $\times$  2 mm  $\times$  10 mm. Spectrographic and vacuum fusion analyses revealed the following impurities in ppm: Ca < 50; Mg < 200; Fe < 100; Ta  $\leq$  1000; Y < 100; Tb  $\leq$  100; Eu < 10; Sm  $\leq$  200; Al,

<sup>11</sup> M. Griffel, R. E. Skochdopole, and F. H. Spedding, *Phys. Rev.* **93**, 657 (1954).

<sup>12</sup> R. V. Colvin, S. Legvold, and F. H. Spedding, *Phys. Rev.* **120**, 741 (1960).

<sup>13</sup> H. E. Nigh, *J. Appl. Phys.* **34**, 3323 (1963).

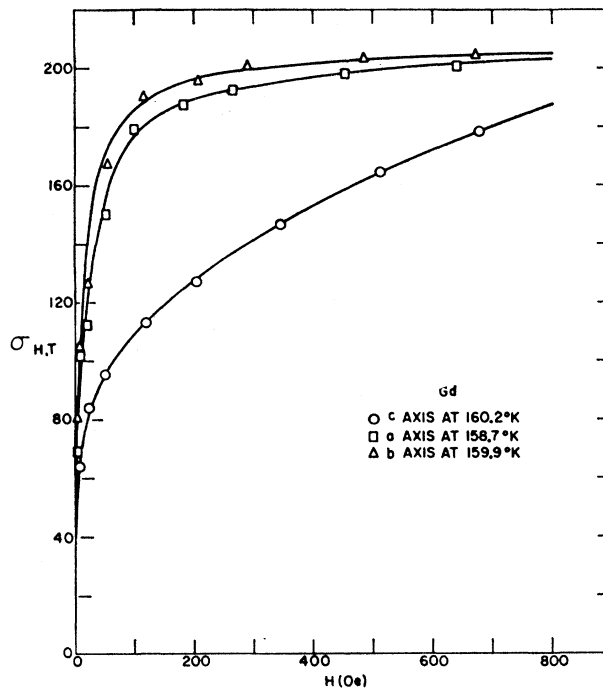


FIG. 2. Magnetic moment per gram versus internal magnetic field for the  $a$ -,  $b$ -, and  $c$ -axis crystals.

Cu, Ni, Si, W present as trace impurities;  $O_2 \approx 950$ ;  $H_2 \approx 5$ ;  $N_2 \approx 120$ .

The experimental procedure for the magnetic measurements from 1.4 to 350°K was the same as that described by Strandburg *et al.*<sup>14</sup> A standpipe furnace was constructed to replace the cryostat in the range

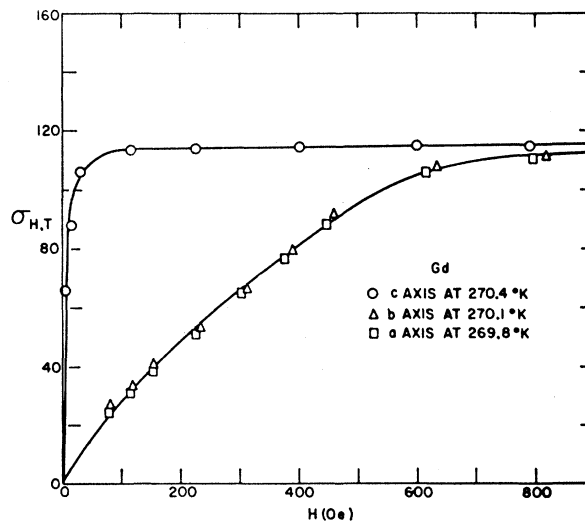


FIG. 3. Magnetic moment per gram versus internal magnetic field for the  $a$ -,  $b$ -,  $c$ -axis crystals.

<sup>14</sup> D. L. Strandburg, S. Legvold, and F. H. Spedding, *Phys. Rev.* **127**, 2046 (1962).

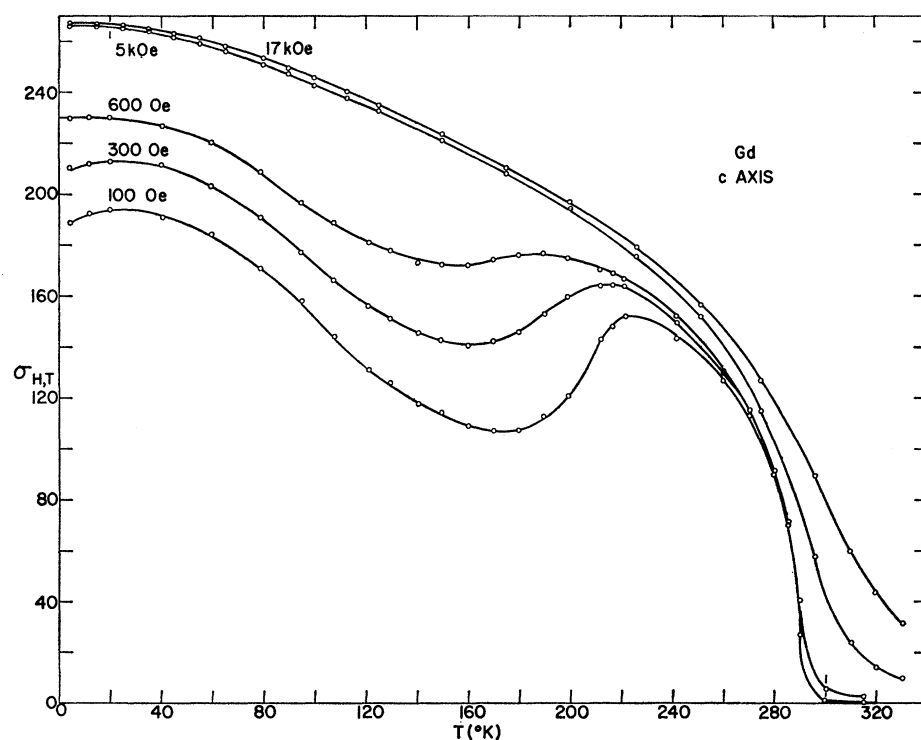


FIG. 4. Magnetic moment per gram versus temperature for the *c*-axis crystal. Internal magnetic fields are indicated.

300 to 900°K. Temperatures were measured in the 300 to 900°K range with a calibrated chromel-alumel thermocouple. Absolute temperature values were determined to  $\pm 2^\circ\text{K}$  in the 300 to 900°K range, while the temperature variation during each series of measurements of the susceptibility at 12, 15, and 18 kOe was controlled to  $0.1^\circ\text{K}$ . The magnetic-field gradient was calibrated in fields from 0 to 6 kOe with Permalloy 78. High-purity iron with an assumed saturation magnetic moment of 217.75 cgs units/g at 293°K was used to calibrate the gradient in fields from 4 to 18 kOe.

Standard four probe electrical resistivity measurements were made on the *c*-axis and *b*-axis crystals from 4.2 to 380°K. The apparatus used for these measurements has been described by Colvin *et al.*<sup>12</sup>

#### EXPERIMENTAL RESULTS

Representative low-field isotherms are exhibited in Figs. 1–3. Isofield curves, constructed from isotherms, are shown in Figs. 4 and 5. The low-field data ( $H < 1000$  Oe) are somewhat qualitative due to the uncertainty in the demagnetizing field and also due to the uncertainty in the calibration of the magnetic field gradient at these low magnetic fields. The low-field data are reliable to  $\pm 4\%$ . The isothermal data indicate (unfortunately, within experimental error) an apparent small basal plane anisotropy in low magnetic fields from 4.2 to about 240°K. Isofield data for the *a* axis are not shown since these data exhibit the same temperature dependence as that shown in Fig. 5 for the *b* axis.

Figures 1–3 show how the variation of the easy direction of magnetization with temperature affects the magnetization in the symmetry directions. At 4.2°K, the magnetization vector is about  $30^\circ$  from the *c* axis; at 160°K, the magnetization vector is very close to the basal plane; while at 270°K, the magnetization vector is parallel to the *c* direction.<sup>8,9</sup> The *c*-axis isofield curves of Fig. 4 show a peak at 220°K and a broad minima at 160–180°K at low fields. The *b*-axis isofield curves of Fig. 5 show a peak at 120°K for low fields. The high-field data shown in Figs. 4 and 5 were also constructed from isotherms and exhibit nearly normal Weiss behavior.

In Fig. 6 the reduced spontaneous magnetization for the *b* axis is plotted as a function of  $T/\theta$ , where  $\theta$  is the Curie temperature. A comparison is made to the theoretical curves for  $J = \frac{1}{2}$  and  $J = \infty$  in the Weiss theory of ferromagnetism. The spontaneous magnetization data were determined by linear extrapolation of the isotherms to  $H = 0$  for temperatures from 4.2 to 225°K. Above 225°K the spontaneous magnetization was determined by plotting  $\sigma^2$  versus  $H/\sigma$  and extrapolating from the high-field region to  $H = 0$ .

In Fig. 7 are shown representative plots of the magnetic moment per gram as a function of  $1/H$  for the *c*- and *a*-axis crystals. The saturation moments,  $\sigma_{\infty, T}$ , were obtained by extrapolating these curves to infinite fields. In Fig. 8 the saturation moments are plotted versus  $T^{3/2}$  for temperatures from 4.2 to 250°K, and versus  $T^2$  for temperatures from 4.2 to 80°K. The

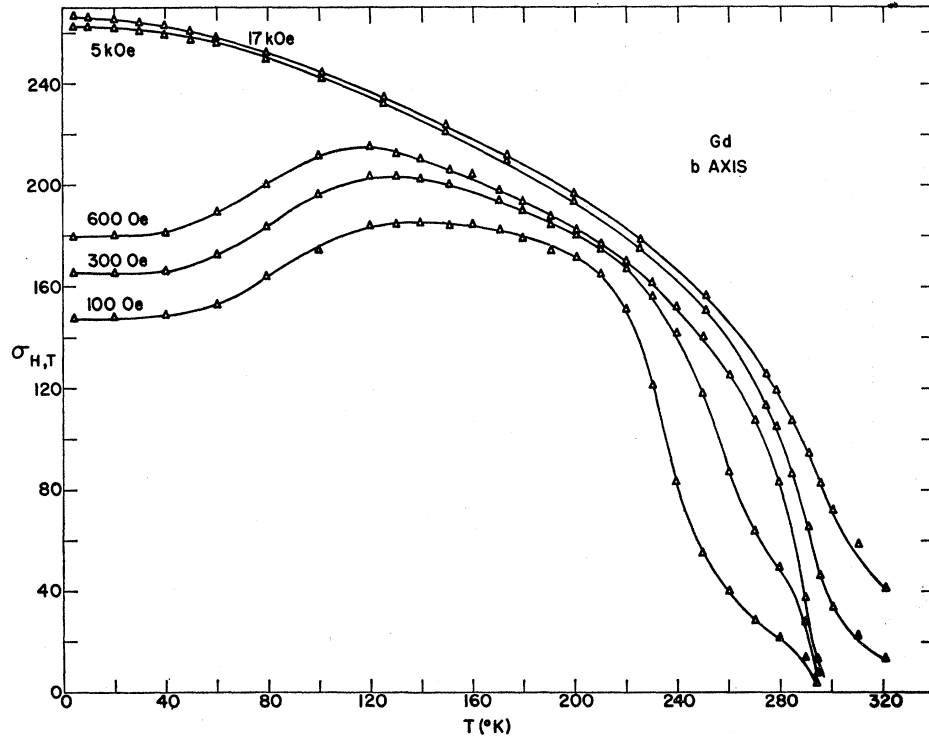


FIG. 5. Magnetic moment per gram versus temperature for the *b*-axis crystal. Internal magnetic fields are indicated.

experimental data fit the  $T^{3/2}$  law to  $\pm 0.1\%$  from 50 to about 200 $^{\circ}\text{K}$ . The data deviate from  $T^{3/2}$  behavior below 50 $^{\circ}\text{K}$  and, as shown in Fig. 8, fit the  $T^2$  law rather well; although a log-log plot of the low-temperature data indicated the behavior as  $T^{2.2 \pm 0.1}$ . There is a small anisotropy in the saturation moment as can be seen in Figs. 7 and 8, however the data for the *a* axis are nearly coincident with those for the *c* axis below

50 $^{\circ}\text{K}$ . For the *c* axis, the absolute saturation moment,  $\sigma_{\infty,0} = 268.4 \pm 0.5$  cgs units/g which is equivalent to  $7.55 \pm 0.02$  Bohr magnetons/atom. The absolute saturation

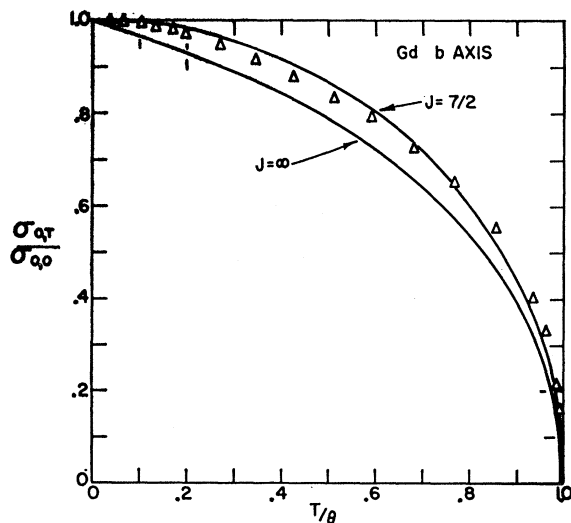


FIG. 6. The reduced spontaneous magnetization curve for the *b*-axis crystal. The solid lines are for  $J = \frac{7}{2}$  and  $J = \infty$ , from the Weiss quantum theory of ferromagnetism.

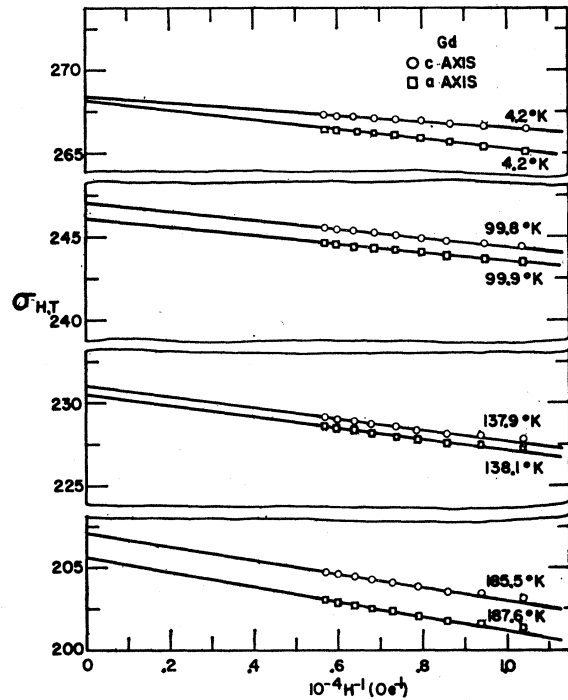


FIG. 7. Magnetic moment extrapolations to infinite field for the *c*- and *a*-axis crystals.

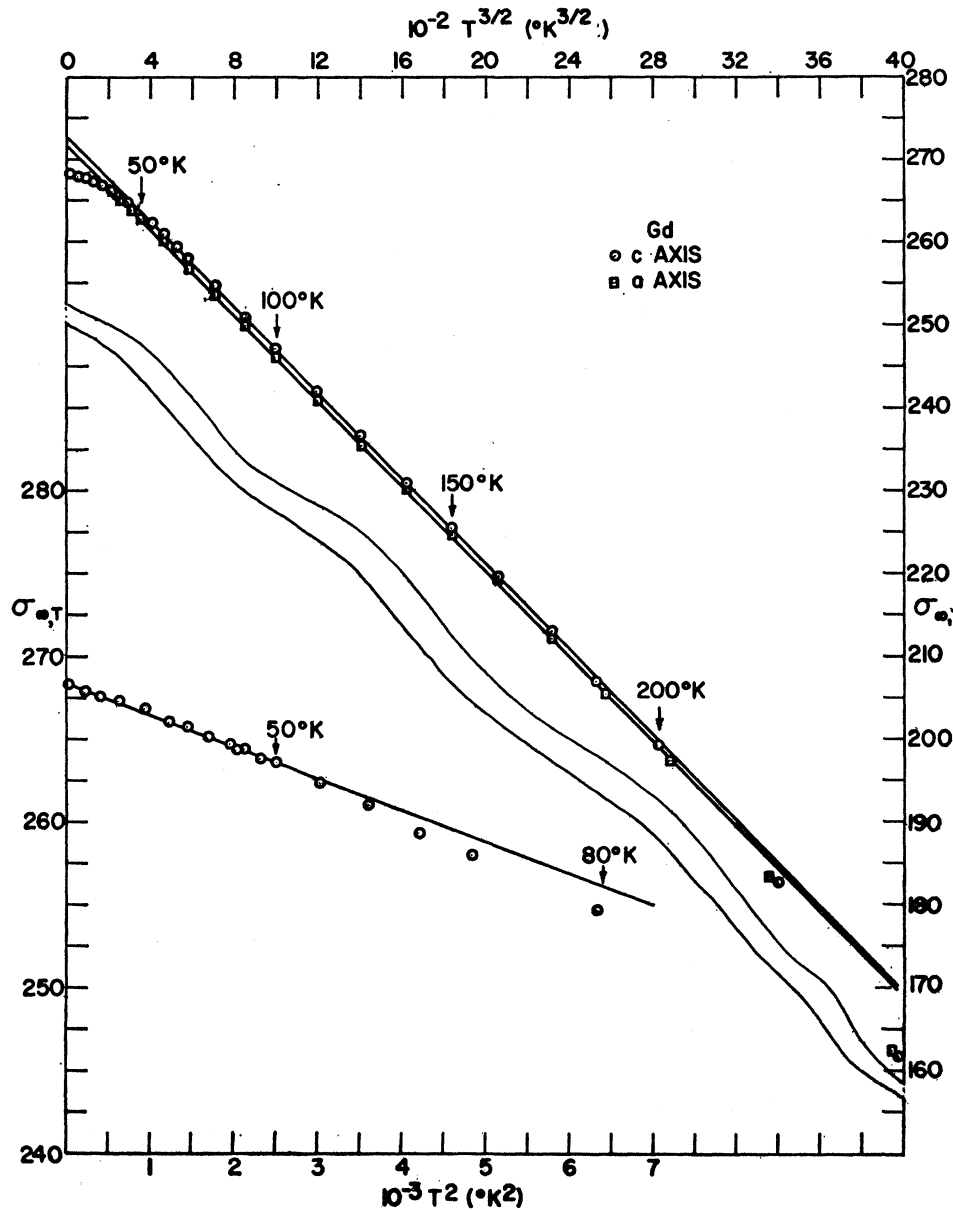


FIG. 8. The saturation magnetic moment as a function of  $T^2$  and  $T^{3/2}$ .

tion moment for the  $a$  axis is  $\sigma_{\infty,0} = 268.2 \pm 0.5$  cgs units/g. The saturation values are taken from a  $T^2$  plot and are to be compared with the theoretical saturation moment of  $gJ = 7.0$  Bohr magnetons for the  $^8S_{7/2}$  state for the ion, which does not include conduction electron effects.

Figure 9 is a plot of the reciprocal of the magnetic susceptibility,  $1/\chi$ , as a function of temperature. Curie-Weiss behavior was observed from 400 to 900°K. No anisotropy was observed in the paramagnetic region. The experimentally determined paramagnetic Curie temperature is  $317 \pm 3^\circ\text{K}$  and the effective Bohr magneton number is  $7.98 \pm 0.05$ , in good agreement with the theoretical value of  $\mu_{\text{eff}} = g[J(J+1)]^{1/2} = 7.94$ .

The electrical resistivities (residual subtracted) of the  $b$ - and  $c$ -axis crystals are displayed in Fig. 10 as a function of temperature. The inserts show the behavior in the vicinity of the Curie point. The change in slope for the  $b$ -axis curve occurs at  $293.2 \pm 0.2^\circ\text{K}$ . The  $c$ -axis curve shows a rounded maximum at about  $292^\circ\text{K}$  and a shallow minimum at about  $340^\circ\text{K}$ . No thermal hysteresis was observed in the vicinity of the Curie point.

#### DISCUSSION

Magnetic anisotropy was observed in Gd below the Curie temperature. The low-field studies confirm that the easy direction of magnetization is a function of

temperature and are in qualitative agreement with the torque measurements.<sup>8,9</sup>

The experimentally determined absolute saturation moment of  $7.55\mu_B$  is in excess of the theoretical moment by  $0.55\mu_B$ . Liu<sup>15</sup> has suggested that polarization of the conduction electrons may be responsible for the excess moment. It is not believed that the departure from  $T^{3/2}$  behavior at low temperatures could arise from an energy gap.<sup>16</sup> On the other hand, it is conceivable that some mechanism associated with the conduction electrons could give rise to such an effect.

The observed  $T^{3/2}$  dependence of the saturation magnetization has been explained by Goodings<sup>17</sup> as due to a complicated cancellation of higher order effects.

The ferromagnetic Curie temperature was determined from a  $\sigma^2$  versus  $H/\sigma$  plot and was found to be  $293.2 \pm 0.4^\circ\text{K}$ . This temperature is in good agreement with the change in slope at  $293.2 \pm 0.2^\circ\text{K}$  observed for the *b*-axis resistivity curve.

No anomalous behavior was observed in the susceptibility at  $750^\circ\text{K}$ , as reported by Arajs and Colvin.<sup>6</sup>

The behavior of the *c*-axis resistivity above the Curie temperature may be due to short-range order which persists up to at least  $340^\circ\text{K}$ . This conclusion is supported by the departure of the susceptibility from Curie-Weiss behavior below  $400^\circ\text{K}$  as shown in Fig. 9. In addition, the torque measurements of Graham<sup>8</sup> show an apparent anisotropy, which is strongly field-dependent, above the Curie temperature. Bozorth and

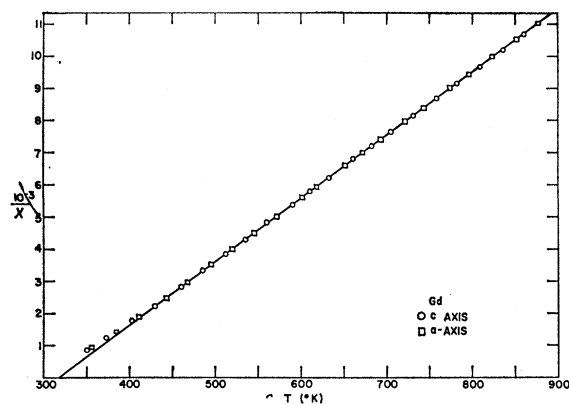


FIG. 9. Inverse paramagnetic susceptibilities of the *c*- and *a*-axis crystals as a function of temperature.

<sup>15</sup> S. H. Liu, Phys. Rev. **123**, 470 (1961).

<sup>16</sup> K. Niira, Phys. Rev. **117**, 129 (1960).

<sup>17</sup> D. A. Goodings, Phys. Rev. **127**, 1532 (1962).

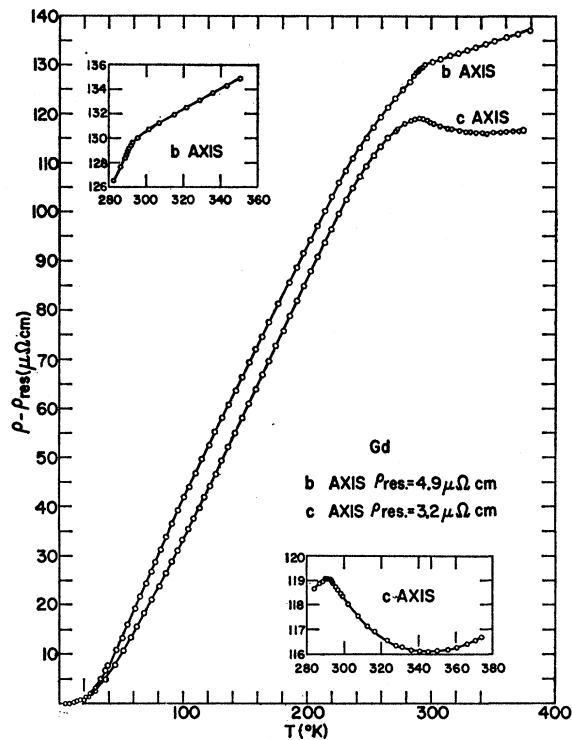


FIG. 10. Electrical resistivity, residual subtracted, versus temperature for the *c*- and *b*-axis crystals. The inserts are enlargements of the data near the Curie point.

Wakiyama<sup>18</sup> observed anomalous behavior in the forced magnetostriction near the Curie temperature.

It was found that a good fit to the experimental data on polycrystalline Gd of Colvin *et al.* was achieved by the use of the relationship  $\rho_{\text{poly}} = \frac{1}{3}(2\rho_b + \rho_c)$ , where  $\rho_b$  is the *b*-axis resistivity,  $\rho_c$  is the *c*-axis resistivity, and  $\rho_{\text{poly}}$  is the calculated polycrystalline resistivity. Alstad *et al.*<sup>19</sup> have verified this relationship for yttrium.

#### ACKNOWLEDGMENTS

The authors wish to thank C. Habermann and P. Palmer for preparing the gadolinium metal. S. Arajs of the U. S. Steel Corporation kindly provided the high-purity iron used for calibration of the magnetic-field gradient.

<sup>18</sup> R. M. Bozorth and T. Wakiyama, J. Appl. Phys. **34**, 1351 (1963).

<sup>19</sup> J. K. Alstad, R. V. Colvin, and S. Legvold, Phys. Rev. **123**, 418 (1961).